Biodegradation **9:** 443–449, 1998.

An application of nuclear magnetic resonance imaging to study migration rates of oil-related residues in estuarine sediments

J.A. Chudek[1*] & A.D. Reeves[2]
[1] *Department of Chemistry,* [2] *Department of Geography, University of Dundee, Dundee DD1 4HN, Scotland, UK (*author for correspondence)*

Key words: anthropogenic contamination, magnetic susceptibility artefacts, marine sediment, MRI, oil

Abstract

Organisations such as the Marine Control Pollution Unit of the Department of Transport are at present testing the suitability of burial and landfarming of oily residues in sandy coastal environments as an alternative to landfill sites. The tendency for oil related compounds to sorb to sediments has been extensively investigated, but this has not permitted the 'observation' or measurement of advection/diffusion processes or the breakdown of these compounds within sediments.

MRI, which is a multidimensional technique allowing the position of nuclei (most commonly protons) to be charted within a volume, provides a means of monitoring advection and diffusion of oil within sediments, thus offering a method of assessing the harming potential of oils in near-shore environments. A three dimensional MRI analysis of the movement of oil in an organic substrate and in three related estuarine sediments show that, using appropriate parameters, movement of the oil can be both observed and quantified. The results presented in terms of the % change of oil distribution within each sediment sample, show the great potential of MRI in studying protonated contaminants in these materials.

Introduction

While magnetic resonance imaging (MRI) is possibly still best known for its enormous contribution to diagnostic medicine it has, over the last decade or so, been used in a great variety of scientific disciplines. One major use has been in the non-invasive study of the movement of liquids in a wide range of materials. Callaghan (1991) discusses many of these applications and describes how the presence of paramagnetic materials, air spaces, liquid/air and liquid/liquid interfaces can all potentially wipe out MRI images by perturbing the linear magnetic field gradients used in imaging to an extent that the images become meaningless. He shows that these susceptibility effects are in the frequency domain and finite. The use of large sweepwidths and high magnetic field gradient strengths, while not eliminating these effects, can minimise them (Callaghan 1991). Increasing the sweepwidth also enables lower echo times to be used, decreasing the lower T_2 'cutoff limit', and consequently allowing more protons to be observed. The knowledge of the presence of magnetic susceptibility effects has led many to ignore conventional MRI as a tool in the study of movement in substances such as marine sediments or soil from polluted industrial sites. As a possible consequence of this, the application of NMR, including MRI, to the assessment of anthropogenic contamination is an important area in which research activity is still at a moderate level.

MRI has been shown to be an ideal method for the analysis of fluid flow in a variety of environmental substrates. Borgia (1994) reviews the 'explosive growth' in MRI techniques which are being applied to a diverse range of studies involving fluids in heterogeneous or model systems. More specifically, MRI is at present being used to map the position of oil in rock cores and it can also be used to approximate the relative concentrations of oil and water (Davies et al. 1994). MRI has been used to obtain porosity distribu-

tions and fluid flow velocities by measuring localised porosity values inside natural porous rocks (Williams & Taylor 1994; Fordham et al. 1994; Amin et al. 1994, 1996; McDonald et al. 1996 and McDonald 1996). The ability of MRI to image oil in the various rock cores show that susceptibility effects in sediments need not necessarily be a major problem.

MRI is shown here to be an important method for quantitatively assessing diffusion and advection of oil in marine sediments hence offering the opportunity to determine the harming potential, in terms of the spread, of pollutant oils in the coastal marine environment. It is intended that this analytical protocol could be used for calculating the extent to which longer term remedial action is required when oil residues reach coastal areas, by allowing the effects of pollution incidents to be understood in greater detail. This is of particular relevance when the rates of biodegradation of weathered oily residues need to be monitored *in situ*. The work is timely in that organisations such as the Marine Control Pollution Unit of the Department of Transport are testing the suitability of burial and landfarming of oily residues in sandy coastal environments as an alternative to landfill sites (Harrison 1995).

Four samples were analysed, one of peat, which is high in organic material and low in paramagnetic species, and consequently ideal for MRI, and three samples of sediment, gathered from differing parts of the estuary of the River Tay in east Scotland. These sediments contain various percentages of sand, silt and clay, and traces of paramagnetic substances, including 3% Fe, normally considered difficult to image. Each sample had a small aliquot of oil added before imaging over a set time period. Images were acquired applying Callaghan's (1991) criteria, using the spectrometer's longest sweepwidth and the highest practical gradient strengths. The various images were examined and the volume and rates of oil diffusion in each sediment was calculated and compared with that of the others.

Experimental

Sample collection and handling

Peat rich soil. Lyme park, Cheshire, England, UK. Grid Ref. SJ 970 815.
Sediment samples. Three sediment samples were collected from the Tay Estuary.
A. Broughty Ferry Beach: Grid Ref. OS 477 312
B. Monifieth Beach: Grid Ref. OS 487 316
Collected by scooping sediment exposed at low tide to a depth of 5 cm.
C. Invergowrie Bay: Grid Ref. OS 357 297

These were collected using a grab sampler, of modified van Veen design (0.25 m^3 volume) with added teeth to collect sediment more effectively (commissioned by the Tay Estuary Research Centre, Old Ferry Pier, Newport on Tay, Fife). The grab penetrates bottom sediments to a depth of approximately 10 cms. All samples were collected and returned to the laboratory for immediate use.

Samples were examined in the MR imager with no pre-preparation. An inert plastic container (15 mm diam., 24 mm length) was part filled with damp sediment. A 5 mm diam. cotton wool ball, soaked in Shell Corena oil, was placed on the sediment surface. The container was totally filled, covering the cotton wool. It was subsequently placed in a 25 mm od glass tube and inserted into the magnet. Image data collection was started immediately.

NMR imaging experiments

All ^{1}H images were recorded using a Bruker AM300/WB Fourier Transform spectrometer equipped with a Bruker microimaging accessory fitted with a 25 mm diameter saddle coil. A standard Bruker 3D spin-echo pulse sequence was used to collect data (Bruker XY3DSE). The data matrix size was: 256 $\times$ 128 $\times$ 128 for the 3D accumulation. With a field of view of 25 $\times$ 25 $\times$ 25 mm this gave a voxel (the smallest cubic unit the image divides into) resolution of 195 $\times$ 195 $\times$ 195 μm.

Data was collected using the following parameters: repetition time (TR), 1.0 s; time to echo (TE), 4.2 ms; sweep width, 100,000 Hz; number of transients, 2; total acquisition time per experiment, 9 h. Gradient strengths were calculated to give the required field of view at that sweepwidth.

The data were transformed and worked up on a Bruker Aspect X32 work station. After Fourier Transformation the data points that lay outwith the region of interest (the part containing the volume of contaminated sediment) were deleted giving a cube of 80 $\times$ 80 $\times$ 80 voxels, this matrix was then interpolated up to a data matrix with 192 voxels on a side, making the voxel size 83 μm per side. This allowed slices through the data to be examined individually (see results). As a means of making the data more visually meaningful, a type of 3D data reconstruction known

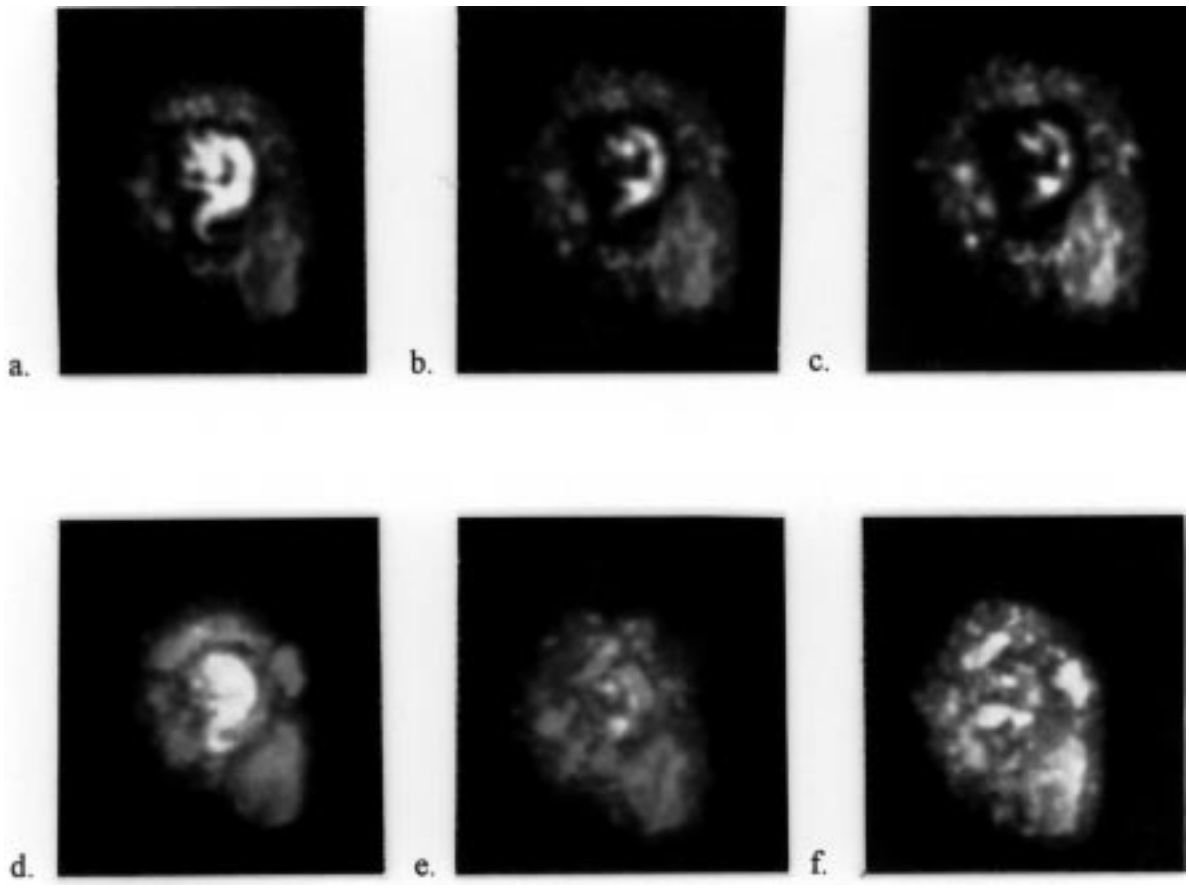

Figure 1. Magnetic resonance images of a sample of peat contaminated with oil. a–c: Central slice through the data set showing the oil distribution; a, on mixing; b, after 18 h and c, after 36 h. d–f: View of the maximum intensity projections of the full data sets used in a–c illustrating the oil movement in all directions.

Table 1. Volume of sediment occupied by oil 32 hours after addition and changes in oil distribution

Sample	Volume of sediment occupied by oil μm^3	Volume in which oil concentration increases (%)	Volume in which oil concentration decreases (%)
A	6.8×10^{10}	10	9
B	3.4×10^{10}	23	89
C	2.6×10^{11}	30	10

as a maximum intensity projection was formed from each data set. In this, the regions of maximum proton intensity are depicted as white, shading through various levels of translucency with lowest intensities being transparent. This allows the region of contamination to be examined from all directions on a screen.

Although these experiments were not carried out using a standard sample, which might have allowed any apparent changes in the mass of the oil to be calculated, an integral of the total signal intensity of each image in the time course of the experiment enabled relative changes taking place in the contaminated sample, with time, to be observed. Changes in the spatial distibution of oil over time was monitored by comparing the relative intensity of each voxel in two images, one recorded at time zero (T_0) and one recorded after

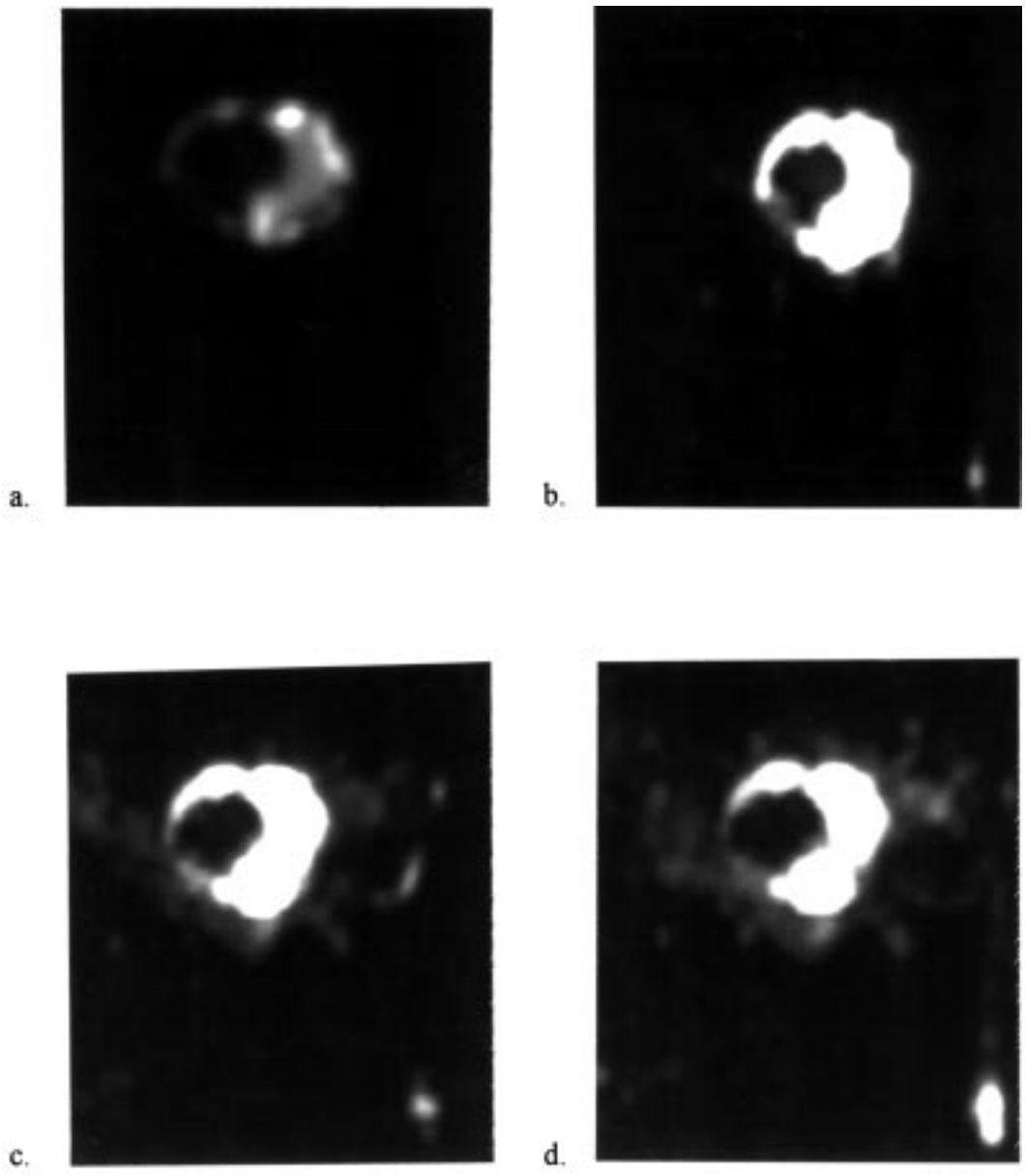

Figure 2. Magnetic resonance images of sediment sample B (Monifieth) contaminated with oil. a: The central slice through the data set showing the oil distribution on mixing; b, the same image with the intensity increased; c, after 18 and d, after 36 h, illustrating the diffusion of oil into the sediment.

x hours (T_x), and constructing a plot of the intensity of the voxels from the image at T_0 vs. those of the image at T_x. Any deviation from the diagonal can be taken to signify *relative* changes in intensity caused by movement of the contaminant away from or towards the region containing these voxels. Further manipulation of the data enables pseudo-3D reconstructions of the volumes loosing intensity, the volumes increasing in intensity and volumes of unchanged voxels to be made as surface reconstructions and again examined by eye on a screen. It further counts these voxels so that the changes in volume can be quantified. Changes in volume are given as 100 × No. of voxels where intensity increases (or decreases)/Total no. of voxels showing contamination.

The acquisition parameters used were found in preliminary experiments to maximise contrast and minimise susceptibility artefacts.

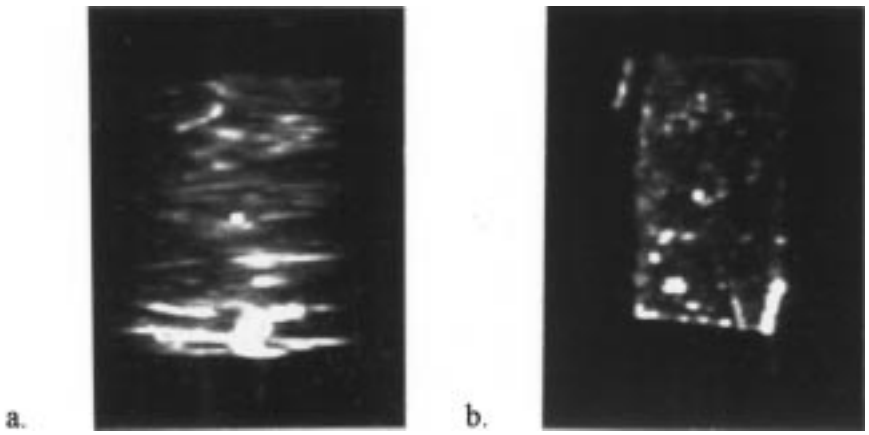

Figure 3. Maximum intensity projection images of a sediment/oil mixture illustrating magnetic susceptibility artefact 'streaking' in the read direction. In image a, the read direction is left to right, in b, the image has been rotated through 90° and the artefacts can no longer be observed.

Particle size analysis

Particle size analyser: Coulter LS230 Laser Analyser with variable speed fluid module. Samples were analysed by adding directly to the Coulter in their original form, i.e. wet sediment with no prior dispersion. This retains the effective, *in situ* particle size characteristics.

Loss on ignition

Loss on ignition: 800 °C for 2 h in a muffle furnace (Mudge and Bebianno 1997).

Results and discussion

The bright areas in the images shown here indicate volumes of the sample contaminated with oil. Image intensity due to water protons is barely above the background noise. It is thought that this low intensity may be explained by partial saturation of the water signal under the experimental conditions used. Any binding of the water to the sediment would tend to further increase T_1, it would also almost certainly shorten T_2, again affecting water signal strength. Figure 1a–c, show the changes seen in the central slice of a 3D spin echo image through a low mineral, highly organic substrate (peat) immediately after the addition of oil (a); 18 h after the addition (b) and (c) after a subsequent 18 h period. As can be clearly seen two forces direct the spread of the oil in this material. In Figure 1a, the oil has initially 'run', under the force of gravity, into the substrate. Figure 1b and c show that forces of advection cause the oil to diffuse in all directions. A pseudo-3D maximum intensity projection of the full data sets for the each image is given in Figure 1d–f. These indicate very clearly a drop in oil concentration in the centre of the spill and the diffusion of the oil into the outer regions.

The initial image of the oil in sediment B accumulated under the same conditions as the peat images (Figure 2a) highlights the ability of MRI to 'observe' organic pollutants in sediments. The most important aspect of this image is that there is no sign of the 'streaking' of the image in the read (left to right) direction which would be associated with susceptibility artefacts (Callaghan 1991). This effect is illustrated clearly in Figure 3a and b. These images are maximum intensity projections of data sets of oil/sediment mixtures accumulated with a sweep width of 25,000 Hz, a quarter of that used for the other data sets, viewed a, with the read direction orientated left to right and b, looking along the read axis. In Figure 2a, it is difficult to determine if there has been a 'run' of oil similar to that in the peat sample. It does appear likely that there has been some movement, as the oil was added as a single mass and the image shows what must have been a rapid dispersion about a relatively oil free region. Figure 2b, shows the same image but in this print the intensity has been increased to highlight the background, which is comparatively oil free. If this image is compared with those shown in Figure 2c and d, which are of the same sample after 18 and 36 h respectively, definite indications of diffusion can be observed. Again as with the peat, diffusion is in all directions. It is interesting that the oil only shows in 'pockets' as if it is being concentrated in these areas,

Table 2. Characteristics of the sediments

Sample	Loss on ignition (%)	Sand (%)	Silt (%)	Clay (%)
A	1.25	100	0	0
B	2.49	68.8	29.2	2.0
C	2.05	75.2	23.3	1.5

whilst in the intervening regions the concentration is too low to be observed.

Similar images (not shown) were accumulated for the other two sediments after treatment with oil. All Images were analysed using the Bruker UXNMR software, the results of this analysis are shown in Table 1. Table 2 gives the physical properties of each of these sediments.

It is in the examination of the data derived from the measurement of voxel intensities between the different images, in a time sequence, that real information about the interactions of oil contamination with sediments begins to emerge. The distribution of values found on integration of the signal intensity for each of the images accumulated in the various time sequences shows a variation of less than 5%. This might indicate that there is very little adsorption of the oil onto the particles of the sediment, which would almost certainly lead to a further reduction in T_2, and a drop in image intensity, and that it is displacement that is being observed. The values shown by the integration also gives credence to results based the comparison of the individual images in each time sequence. In Table 1, column 1, it can be seen that in the initial image the volume of contamination varies considerably. This volume change may correlate with the sources of the sediment, in that the spread of oil contamination within the volume of each sample increases as the distance of the collection site from the mouth of the estuary increases. Columns 2 and 3 show the relative movement of oil concentration (as related to voxel intensity). As might be expected these results show that for sediments A and C the oil is slowly diffusing outwards each at a different rate, leaving a volume where the concentration slowly decreases. The results for sediment B, Figure 2, show that while, the oil is indeed spreading there would appear to be an appreciable volume of sediment where oil is being concentrated, a net inward flow.

Closer examination of the sediment characteristics shown in Table 2 may go part way to explaining the difference in behaviour of the oil within the sediments. Although different experimental regimes were applied, our results conform to the findings of Means et al. (1980). They state that, in the vicinity of an oil discharge or spill, organics of limited water solubility, are expected to rapidly associate with suspended and bedded sediment particles. In areas where sediments have high binding capacities i.e., are organic rich and fine grained, then hydrocarbons may concentrate to levels far exceeding those of the polluted water column.

Conclusion

MRI gives a means of quantitatively assessing diffusion and advection of oil in marine sediments and hence offers a method of determining the harming potential of pollutant oils in coastal marine environments. Magnetic susceptibility effects caused by paramagnetic species and metals, which have hitherto hindered the use of MRI in the study of sediments, can be minimised by setting appropriate instrumental acquisition parameters. The use of MRI gives direct information on flow and diffusion rates, conventional methods of analysis have not permitted this. Moreover, it allows volumes in which contamination has become concentrated to be examined.

References

Amin MHG, Hall LD, Chorely RJ, Carpenter TA, Richards KS & Bache BW (1994) Magnetic resonance imaging of soil-water phenomena. Mag. Res. Imag. 12(2): 319–321

Amin MHG, Richards KS, Chorely RJ, Gibbs SG, Carpenter TA & Hall LD (1996) Studies of soil-water transport by MRI. Mag. Res. Imag. 14(7–8): 879–882

Borgia GC (1994) The many facets of current work in nuclear magnetic resonance for fluids in heterogeneous systems. Mag. Res. Imag. 12(2): 163–165

Callaghan PT (1991) Principles of Nuclear Magnetic Resonance Microscopy. Clarendon Press, Oxford

Davies S, Harwick A, Roberts D, Spowage K & Packer KJ (1994). Quantification of oil and water in preserved reservoir rock by NMR spectroscopy and imaging. Mag. Res. Imag. 12: 394–353

Fordham EJ, Gibbs SJ & Hall LD (1994). Partially restricted diffusion in a permeable

Harrison T. (1995). Disposal of oil contaminated beach materials in sandy coastal environments, NERC News 33: 31

Means JC, Wood SG, Hasset JJ & Banwart WL (1980) Sorption of PAHs by sediments and soils. Environ. Sci. Technol. 16: 93–98

McDonald PJ, Pritchard T & Roberts SP (1996) Diffusion of water at low saturation into sandstone rock plugs measured by broad-line magnetic-resonance profiling. J. Colloid Interface Sci. 177(2): 439–445

McDonald PJ (1996) The application of broad-line MRI to the study of porous media. Mag. Res. Imag. 14(7–8): 807–810

Mudge, SM & Bebianno, MJ (1997) Sewage contamination following an accidental spillage in the Ria Formossa, Portugal. Mar. Poll. Bull. 34: 61–84

Williams JLA & Taylor DG (1994) Measurements of viscosity and permeability of 2-phase miscible fluid-flow in rock cores. Mag. Res. Imag. 12(2): 317–318